Journal of Solar Energy Research (JSER)

Journal homepage: www.jser.ut.ac.ir

Hierarchical Control Approach for an Autonomous Microgrid including PV Systems to Mitigate the Impacts of Non-Linear Loads

Mohammadian [a],M., Khodadadi [a],A., Hosseinian[a],S.H., Abedi[a],M.

[a] Amirkabir University of Technology, Tehran, Iran.
*E-Mail: a.khodadadi@aut.ac.ir

ARTICLE INFO

Received: 9 October 2016
Received in revised form: 14 January 2017
Accepted: 16 January 2017

Keywords:
PV systems; Hierarchal controller; microgrids; non-linear load

A B S T R A C T

In this paper, a control approach for enhancing the characteristics of a microgrid system is presented. This microgrid includes a PV system in its DC link beside a DC/DC convertor as the interface for connecting to the system inverter. Due to this, the dynamics of the PV system is also considered. The capability of this control system in maintaining the significant feature of system signals under non-linear load or load variation is also investigated. The secondary controller in this system is designed to not only restore the system voltage and frequency but also preserve the value of active and reactive power before and after its operation. The simulation results show the capability of this control system in maintaining the system performance.

1. Introduction

Due to the unprecedented rate of growth in environmental and economic problems, nowadays the expansion of conventional power system plants are doomed to the failure. Therefore, the application of micro grid system has obtained a considerable attention. These systems, thanks to their renewable nature, produce a negligible amount of pollution in comparison to their conventional counterparts. There are numerous approach for realizing this modern system among which PV (photovoltaic) system and wind turbines are the most applicable ones [1, 2].

PV systems are able to satisfy the requirements of outreached areas. The operation of this system is included a simple process in which the output of PV arrays is connected to a DC/DC boost converter which its control commands come from the maximum power point tracking system (MPPT) to extract the optimum power from the installed PV system [3]. Then, this converter is connected to an inverter to transform the DC power to the AC power which can supply the main AC loads. The local loads in the PV systems can be characterized by the non-linear curves like computers, compact florescent lamp and most home appliances. These equipments produce non-linear current which can be transform to non-linear voltage and due to this, it can be harmful for system steady state operation [4].

Operating in grid connected or autonomous mode is one of the significant features of typical microgrids. Normally, when a microgrid is operated in grid connected mode, the operation of micro sources is similar to the constant power sources which means that they are controlled to inject the demanded power in to the network. In islanded mode the micro sources are controlled in order to supply all the demanded power by the local loads while allowed limits for the voltage and frequency is maintained [5, 6].

Most of the DG units have a power electronic interfaces for connecting to the main grid. These interfaces are categorized as follows [7]:

- Current source inverters (CSI) employ inner current loop and PLL for stay synchronized with the main grid. CSIs are mostly used for current injection to the main grid.

- Voltage source inverters (VSIs) consist of inner current loop and outer voltage loop. These converters mostly connected to the storage devices for maintaining the voltage and frequency within the microgrid. CSIs are mainly connected to the small wind turbines and PV systems which needs MPPT algorithms; although these inverters can also operate in VSI modes.

In the conventional power system, the droop control of frequency and voltage is widely employed. Some of the droop control methods for the islanding operation of the microgrid have been used in the literature [8]-[11]. The main advantage of droop control over the centralized control method is that there is no need for high bandwidth communication link and the microgrids can be supported by the DGs regardless of the current resources [12]-[14]. Various researcher efforts have been allocated toward developing and introducing control structure and method to improve the characteristics of the system variable in the presence of renewable resource like PVs. In [15], a special control method for enhancing the power quality of a PV-based microgrid in the presence of non-linear load has been presented. In [16], an autonomous active power control strategy has been proposed for ac-islanded microgrids in order to achieve power management in a decentralized manner. Also in this study, a hierarchical control structure for ac microgrids that is able to integrate the ESS, PV systems, and loads has been proposed.

In this paper, the incremental conductance and integral regulator method is used to extract the maximum power point of the PV system which has been proved its optimal application over conventional algorithm. Also, a special control structure for a decentralized secondary controller is employed to restore the voltage and frequency of the microgrid. The control system for the AC side converter is designed in a way that it can preserve the system nominal condition in the presence of non-linear loads.

The rest of the paper is organized as follow: In the next part the system configuration, PV modeling method and MPPT algorithm are shortly described. Then the hierarchal control structure is stated. The next part shows the capability of the control system in various scenarios by simulation results and the final part is the conclusion.

2. System Configuration

2.1. Case Study Network

Fig. 1 shows the low-voltage under study microgrid. This system is the general form of the distribution system with various loads and DGs connected to a specified feeder. The DG units can be operated either in parallel mode with the main grid or in the autonomous mode for supplying the sensitive loads when the isolating switch is open. In this paper, without losing the generality, the performance of the system under the presence of the two DG units supplying the loads is investigated.

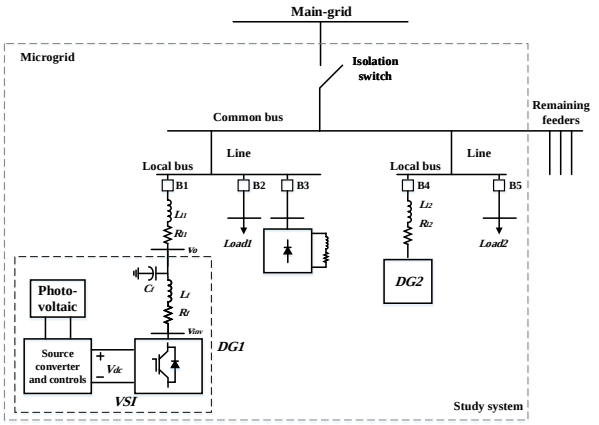

Figure 1: System configuration

The load on the first feeder is inductive. This is a non-linear load with three-phase diode rectifier connected to a R-L load in the DC side. Utilizing a three-phase diode-rectifier for evaluating the performance of proposed controller in rejecting the voltage harmonics of voltage stemming from the non-linear load is recommended.

2.2. PV System

One solar cell is the base unit of a PV module. In the general form, a small solar cell (4 to 6 in^2) produces about 1 to 3 watts electricity. Due to this, for acquiring specific power from a PV system, a combination of series and parallel circuits should be used. By connecting various PV modules in series and parallel configurations, PV arrays are achieved. Obtaining the model of photovoltaic generators, first, its electrical equivalent circuit should be identified. Different mathematical models for describing the non-linear characteristic of the PV cells extracted from the semiconductor junctions have been introduced. The dynamic model of the PV cell is depicted in Fig. 2.

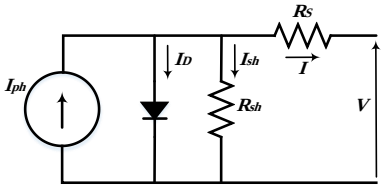

Figure 2 : PV equivalent circuit

The output current of the module is obtained from the below equations.

$$I = I_{ph} - I_D - I_{sh} \qquad (1)$$

$$I = I_{ph} - I_s\left(e^{\frac{q(V+IR_s)}{n1KT}} - 1\right) - \frac{V + IR_s}{R_{sh}} \qquad (2)$$

Where V and I are the *PV* output voltage and current, I_{ph} is the photonic current, I_s is the diode saturation current, q is the Coulomb's constant (1.381e-23 J/K), T is the cell temperature (K), n_1 is the P-N junction ideal coefficient, R_s and R_{sh} are the inherent series and shunt resistors of the cell, respectively. In the ideal PV, R_s=0 (without series dissipation) and R_{sh} = infinity (without ground leakage). In 1 in^2 high quality silicon cell, R_s = 0.05-0.1 Ω and R_{sh}=200-300 Ω. The PV efficiency is sensitive to the small perturbation of the R_s while it's not highly sensitive to the R_{sh} fluctuations. Also, a small increase in R_s will considerably decrease the PV output.

PV arrays specifications, current and power, are simulated in different temperature and radiation levels as

they are shown in Fig. 3 and 4. As it is clear from these figures, the PV array has non-linear voltage-current specification which contains just one single utilization point for obtaining the maximum output power under specific environmental situations.

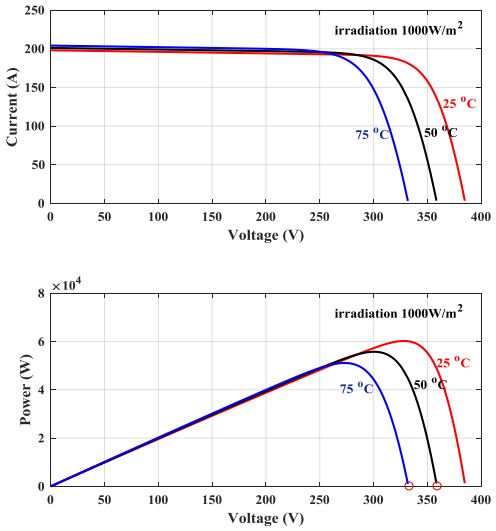

Figure 3 : The PV power in different temperature

2.3. MPPT Algorithm

Maximum power point of a solar array is a point on the I-V characteristic which corresponds to the maximum power of the array (Fig. 4). The main aim of the most MPPT algorithms is to extract and identify this point. Due to the unique feature of this point throughout

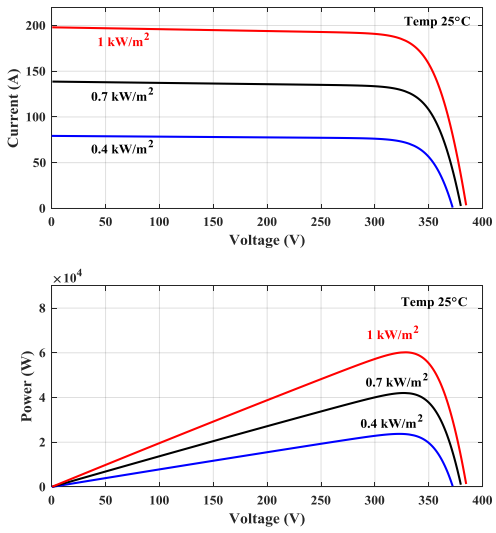

Figure 4 : The PV power in different radiation level

the curve, usually the dp/dv=0 criteria is utilized for pinpointing this point. Mostly the MPPT is implemented on the DC/DC interface between the load and PV. By measuring the current and voltage, the MPPT algorithm using the incremental conductance and integral regulator will find out specific duty cycle for achieving the optimum output power. Fig. 5 depicts the flowchart of this approach for achieving the optimum duty cycle.

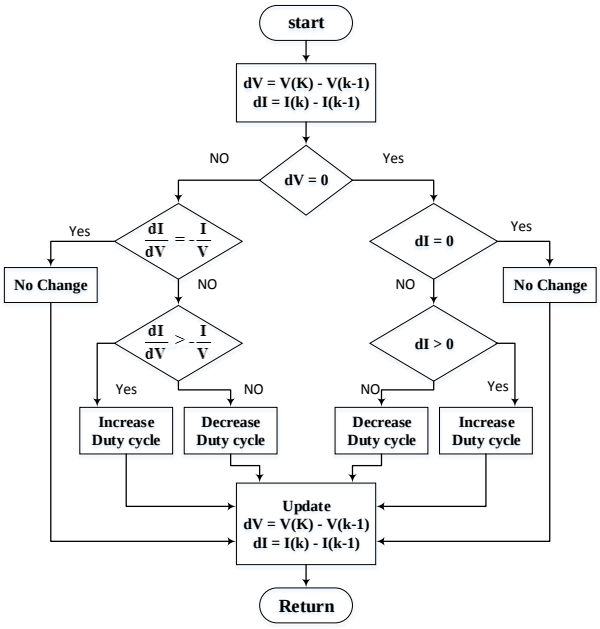

Figure 5 : The flowchart of the MPPT algorithm

2.4. The Boost Convertor

In this study, a boost converter is utilized as an interface for connecting the PV arrays to the DC link capacitor of the inverter. The capacitor connected after PV arrays is mainly used for reducing the high frequency harmonics. This converter is shown in Fig. 6.

3. Control System Architecture

Two distinctive approaches (centralized and decentralized) are identified for power system control architecture:

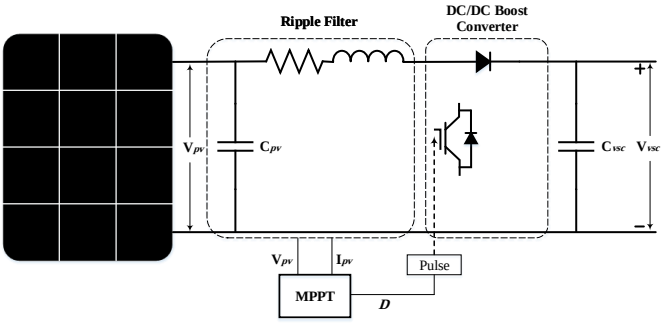

Figure 6 : The boost converter

1) A fully centralized control relies on the data summed up in a central controller that performs required calculations and determines control actions for all units at a single point, requiring huge communication between the central controller and local units.

2) A fully decentralized control which represents units that are controlled by local controllers, only receive local information, and it is not fully aware of system-wide variables and other controllers' actions.

Due to the need for huge communication link and computation burden for interconnected power systems which usually cover extended geographic areas, making the implementation of a fully centralized approach is infeasible. On the other hand, a fully decentralized approach is also not possible due to the strong coupling between the operations of various units in the system, requiring a minimum level of

coordination that cannot be achieved by using only local variables.

A trade-off between fully centralized and fully decentralized control schemes can be achieved by means of a hierarchical control scheme consisting of three control levels. The third level is tertiary which mostly used for planning and management strategies. The primary and secondary levels are described here.

A. Primary Controller

Primary control, also known as the local control (LC) is the first level in the control hierarchy, which have the fastest response between the others. This control is based strictly on local measurements and requires no communication with master controller. Islanding detection, output control and power sharing (and balance) control are the responsibilities of this stage which can be realized by its speed specifications and reliance on local measurements. Power sharing controllers are responsible for the proper sharing of active and reactive power mismatches in the microgrid, whereas inverter output controllers control and regulate output voltages and currents. Inverter output control typically consists of an outer loop for voltage control and an inner loop for current regulation.

As shown in Fig. 7, instantaneous active and reactive power components are calculated from the measured output voltage and output current. These quantities are calculated as:

$$\tilde{p} = v_{od} i_{od} + v_{oq} i_{oq}$$
$$\tilde{q} = v_{od} i_{oq} - v_{oq} i_{od} \quad (3)$$

The instantaneous power components are passed through low-pass filters to obtain the real and reactive powers which is corresponding to the fundamental component.

The frequency is set according to the droop gain and phase is set by integrating the frequency. This imitates the governor action and inertia characteristics of conventional generators and provides negative feedback.

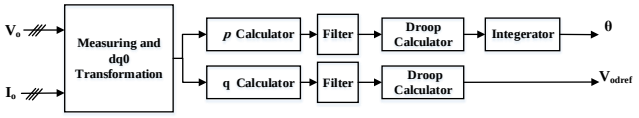

Figure 7: Power controller scheme

For instance, if the power drawn from a generator increases then the rotation of its voltage angle slows and its angle starts decreasing. It is evident that the angle of the inverter voltage, changes in response to the real power flow in the required negative sense and with a gain set by the droop [11].

Voltage Controller

Fig. 8 shows the voltage controller block diagram including all feed-back and feed-forward terms. A PI controller is used for controlling the output voltage.

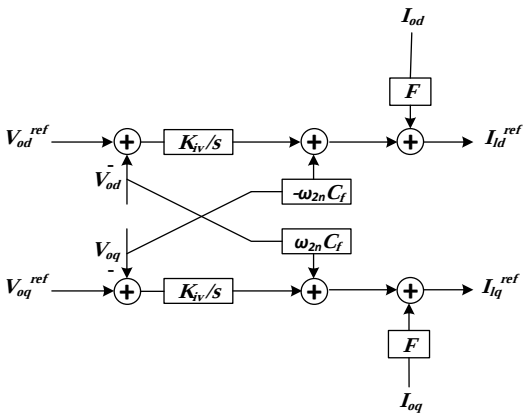

Figure 8 : Voltage controller scheme

Current Controller

Fig. 9 shows the current controller structure. Like the voltage controller, one PI controller is employed for achieving control over output filter inductor current.

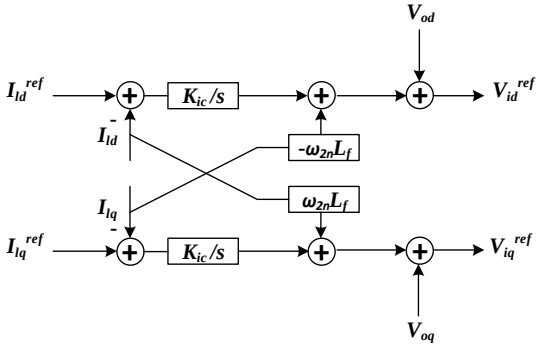

Figure 9 : Current controller scheme

B. Secondary Controller

The main goal of the primary control which is based on local measurements of the output voltage and current, is to calculate *P* and *Q* for the droop method and the virtual impedance control loop. While it is the secondary control action which have the responsibility to restore the rated frequency and voltage.

The secondary control ensures that the rated frequency and voltage are restored by shifting the operating point up to the new curve in which the shared power is maintained. The secondary control would correct grid frequency deviations within allowable limit by employing a proportional–integral (PI)-type controller. The secondary control discussed here is decentralized and performs locally on each DG.

As it is mentioned before, the secondary controller should not change the operation point of the system. Although in this paper an autonomous microgrid is considered and in islanded mode the main purpose of the control system is to maintain the voltage level and frequency within allowable limits, the secondary controller configuration is designed in a way that it can preserve the power sharing level of the system before and after starting its process. Therefore as the input error to the PI controller of secondary controller, we can use:

$$\Delta\omega_{se} = \omega_{rated} - \omega_n + K_{1,se}(P_n - P_m)$$
$$\Delta V_{se} = V_{rated} - V_n + K_{2,se}(Q_n - Q_m) \quad (4)$$

In which, P_m and Q_m are the measured active and reactive power, ω_{rated} and V_{rated} are the nominal frequency and voltage and $K_{1,se}$ and $K_{2,se}$ are the coefficients which balance the difference in power and voltage or frequency. The block diagram of secondary controller is depicted in Fig 10.

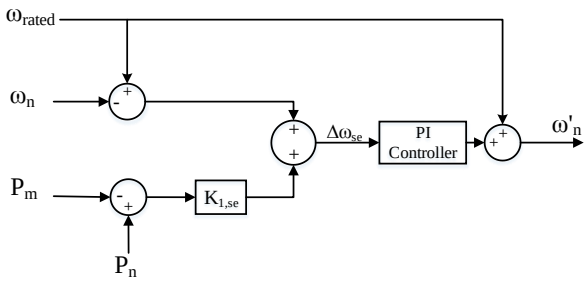

(a)

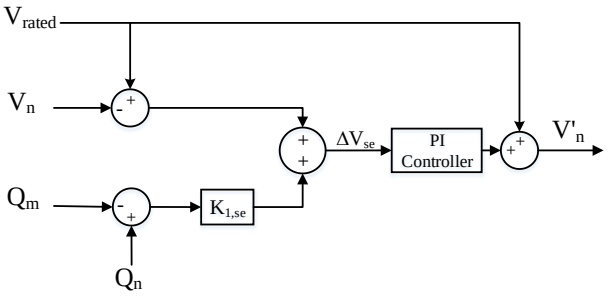

(b)

Figure 10 : Secondary controller (a) Frequency controller (b) Voltage controller

4. Simulation Results and Discussion

For evaluating the control approach, this part states the simulation process and discusses its results on a typical system shown in Fig.1. In this system, two DG units with the proposed control system are utilized which have the capability to work in parallel with the grid. The parameters of the case study system are stated in the Appendix.

Fig. 11 shows the PV output power for evaluating the performance of MPPT algorithm. The irradiance and temperature of the PV which are two important factors on the extracted power of the PV panels are shown in Fig. 11 (a) and (b), respectively. As it is clear in Fig. 11 (c), the lower irradiance level, the smaller output PV power. Also the impact of temperature level on the output power is clear at t=2s, which decrease the power when the temperature is increased. In each mode of operation, MPPT algorithm will adjust the duty cycle in order to extract the optimum active power from the PV. The duty cycle in each moment is shown in Fig. 11 (d).

The performance of the system under sudden change of the load, in this case a non-linear load, is investigated in Fig. 12. Due to the application of the proposed control system in DG1, the non-linear load is installed on the PCC of DG1 and it will start its operation at t=0.9s.

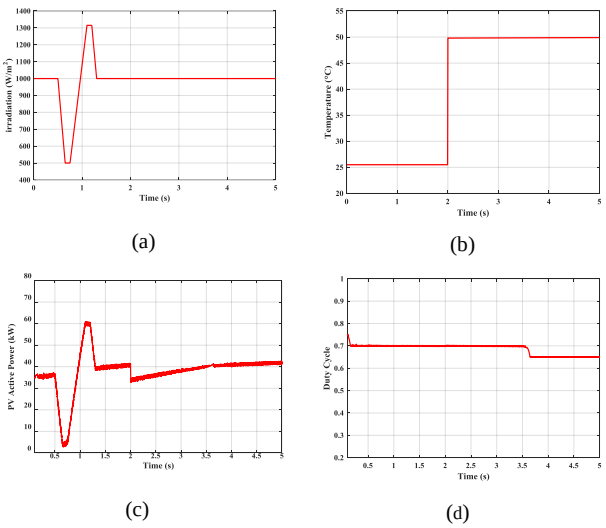

(a) (b) (c) (d)

Figure 11: PV characteristics under irradiation and temperature change (a) Irradiation level (b) Temperature (c) PV active power (d) DC/DC converter duty cycle.

Fig. 12 (a) and (b) show the active and reactive power of each DG before and after the load variation. As it is clear from these figures, each DG is able to supply the scheduled active and reactive power. Because the value of active droop is equal for two DGs, the active power sharing is equal for each of them even after load variation. This power sharing scheme is depicted in Fig. 12 (a) and (b).

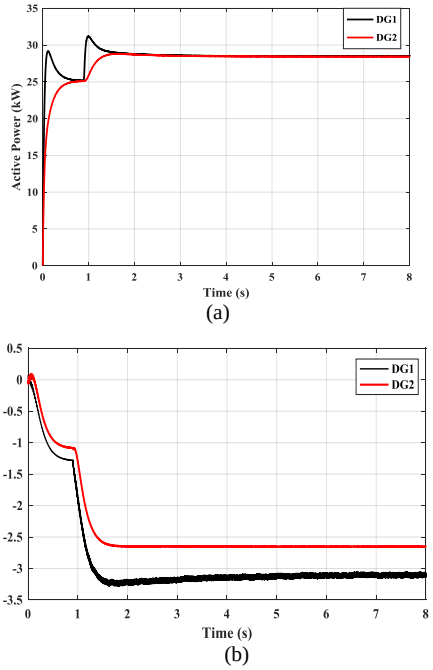

(a)

(b)

Figure 12: DG characteristics before and after load variation (a) Active power (b) Reactive power

One of the main concerns in power system is the power quality issues among which the voltage distortion of the feeding bus is very important. The bus voltage of DG1 is shown in Fig. 13. As this figure shows, the bus voltage even after entering the non-linear load is maintained sinusoidally which shows that the control system is able to preserve the system voltage in non-ideal situation.

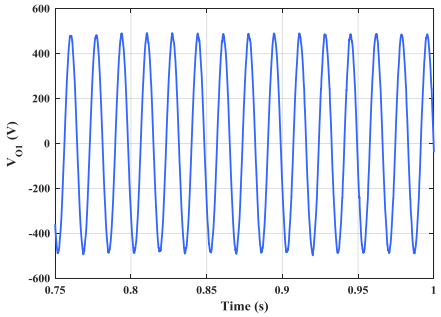

Figure 13: The bus voltage under the non-linear load at t=0.9s

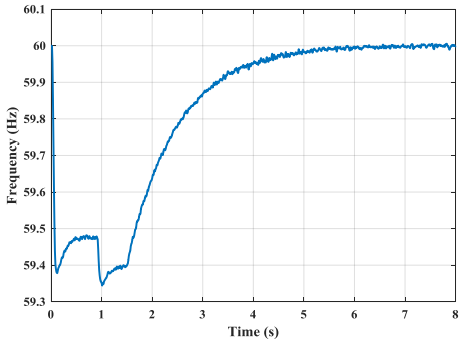

Figure 14: The system frequency

The system frequency is shown in Fig. 14. This frequency is decreased to 59.35 Hz after the sudden change of the load which it is not acceptable in the steady state system operation. Thus, for compensating this value of frequency, like conventional power system, the secondary controller will be employed. The type of applied secondary controller in this paper is decentralized which needs low bandwidth communication which increase the reliability of the system. This controller will restore the system frequency after finishing the primary controller operation. In this paper, the secondary controller is activated at t= 1.5s. The restoration process is depicted in Fig. 14. It should be noted that the operating setpoints of the system should not be changed after activating the secondary controller (Fig. 12 (a), (b)). The operation time of secondary controller is about one minute (or maybe more) depends on the microgrid rating and the number of system elements. The short secondary operation time of our system is due to the number of DGs and lines which have been employed in the system.

5. Conclusions

This paper presents a control approach for enhancing the characteristics of typical microgrid including a PV model for considering the dynamics of DC-link. The cascaded control approach is successfully utilized to eliminate the impacts of non-linear load on the system voltage. In order to restore the system frequency, a special design for secondary controller is utilized to accomplish this restoration. Simulation results excused by MATLAB show the performance of the control system in the presence of non-linear load.

Appendix

Table 1 Parameter of case study system

Type	Parameter		Value
	Symbol	**Quantity**	
tri ca l	V_{dc}	DC Voltage	1.5kV
	V_{MG}	Microgrid Voltage	0.48kV
	f	Microgrid Frequency	60Hz
	C_f	Filter Capacitance	50μF
	L_f	Filter Inductance	1.35mH
	L_o	Output Impedance	0.35mH
	f_s	Switching Frequency	9.9kHz
	r_f	Filter Resistance	0.1Ω
	ω_c	Cut-off Frequency	31.41rad/s
	Load	Resistive load	20/18 kW
	nonlinear load	Resistance	60Ω
		Inductance	10mH
Inner Loops	K_{pv}	Voltage Controller Proportional Term	0.05
	K_{iv}	Voltage Controller Integral Term	390
	K_{pc}	Current Controller Proportional Term	10.5
	K_{ic}	Voltage Controller Proportional Term	16000
	F	Voltage Controller Current Coefficient	0.75
Droop Control	m_p	Active Power Droop	13e-5
	n_q	Reactive Power Droop	1.3e-3
Secondary Controller	K_{pf}	Frequency Proportional Term	0.02
	K_{if}	Frequency Integral Term	1
	K_{pe}	Voltage Proportional Term	0.02
	K_{ie}	Voltage Integral Term	1
	$K_{1,se}$	Active Power Balancing Term	6.13e-4
	$K_{2,se}$	Reactive Power Balancing Term	15.4e-4
Line Parameter	r_l	Resistance of the line	0.012Ω
	L_l	Inductance of the line	29.33mH
	C_l	Capacitance of the line	0.127μF
	L	Line Length	10km

References

[1] B. K. Bose, "Energy, environment, and advances in power electronics," in *ISIE'2000. Proceedings of the 2000 IEEE International Symposium on Industrial Electronics (Cat. No.00TH8543)*, 2000, vol. 1, pp. TU1–T14.

[2] F. Blaabjerg, Z. Chen, and S. B. Kjaer, "Power Electronics as Efficient Interface in Dispersed Power Generation Systems," *IEEE Trans. Power Electron.*, vol. 19, no. 5, pp. 1184–1194, Sep. 2004.

[3] I. Houssamo, F. Locment, and M. Sechilariu, "Experimental analysis of impact of MPPT methods on energy efficiency for photovoltaic power systems," *Int. J. Electr. Power Energy Syst.*, vol. 46, pp. 98–107, 2013.

[4] N. R. Watson, T. L. Scott, and S. Hirsch, "Implications for Distribution Networks of High Penetration of Compact Fluorescent Lamps," *IEEE Trans. Power Deliv.*, vol. 24, no. 3, pp. 1521–1528, Jul. 2009.

[5] R. H. Lasseter, "MicroGrids," in *2002 IEEE Power Engineering Society Winter Meeting. Conference Proceedings (Cat. No.02CH37309)*, 2002, vol. 1, pp. 305–308.

[6] R. Lasseter, A. Akhil, C. Marnay, J. Stephens, J. Dagle, R. Guttromsom, A. S. Meliopoulous, R. Yinger, and J. Eto, "Integration of distributed energy resources. The CERTS Microgrid Concept," Berkeley, CA, Apr. 2002.

[7] J. M. Guerrero, J. C. Vasquez, J. Matas, L. G. de Vicuna, and M. Castilla, "Hierarchical Control of Droop-Controlled AC and DC Microgrids—A General Approach Toward Standardization," *IEEE Trans. Ind. Electron.*, vol. 58, no. 1, pp. 158–172, Jan. 2011.

[8] A. Mehrizi-Sani and R. Iravani, “Potential-Function Based Control of a Microgrid in Islanded and Grid-Connected Modes,” *IEEE Trans. Power Syst.*, vol. 25, no. 4, pp. 1883–1891, Nov. 2010.
[9] M. C. Chandorkar, D. M. Divan, and R. Adapa, “Control of parallel connected inverters in standalone AC supply systems,” *IEEE Trans. Ind. Appl.*, vol. 29, no. 1, pp. 136–143, 1993.
[10] D. De and V. Ramanarayanan, “Decentralized Parallel Operation of Inverters Sharing Unbalanced and Nonlinear Loads,” *IEEE Trans. Power Electron.*, vol. 25, no. 12, pp. 3015–3025, Dec. 2010.
[11] N. Pogaku, M. Prodanovic, and T. C. Green, “Modeling, Analysis and Testing of Autonomous Operation of an Inverter-Based Microgrid,” *IEEE Trans. Power Electron.*, vol. 22, no. 2, pp. 613–625, Mar. 2007.
[[12] B. M. Nomikos and C. D. Vournas, “Investigation of Induction Machine Contribution to Power System Oscillations,” *IEEE Trans. Power Syst.*, vol. 20, no. 2, pp. 916–925, May 2005.
[13] P. Waide and C. U. Brunner, “Energy-Efficiency Policy Opportunities for Electric Motor-Driven Systems,” 2011.
[14] “Standard load models for power flow and dynamic performance simulation,” *IEEE Trans. Power Syst.*, vol. 10, no. 3, pp. 1302–1313, 1995.
[15] N. D. Nguyen Duc Tuyen and G. Fujita, “PV-Active Power Filter Combination Supplies Power to Nonlinear Load and Compensates Utility Current,” *IEEE Power Energy Technol. Syst. J.*, vol. 2, no. 1, pp. 32–42, Mar. 2015.
[16] Wu, Dan, Fen Tang, Tomislav Dragicevic, Juan C. Vasquez, and Josep M. Guerrero. "Autonomous active power control for islanded ac microgrids with photovoltaic generation and energy storage system." *IEEE Transactions on Energy Conversion* 29, no. 4 (2014): 882-892.
[17] M. G. Villalva, J. R. Gazoli, and E. R. Filho, “Comprehensive Approach to Modeling and Simulation of Photovoltaic Arrays,” *IEEE Trans. Power Electron.*, vol. 24, no. 5, pp. 1198–1208, May 2009.